



## Multi-scale analysis of hypochlorite induced PES/PVP ultrafiltration membranes degradation

Bastien Pellegrin, Romain Prulho, Agnès Rivaton, Sandrine Thérias, Jean-Luc Gardette, Emmanuelle Gaudichet-Maurin, Christel Causserand

### ► To cite this version:

Bastien Pellegrin, Romain Prulho, Agnès Rivaton, Sandrine Thérias, Jean-Luc Gardette, et al.. Multi-scale analysis of hypochlorite induced PES/PVP ultrafiltration membranes degradation. *Journal of Membrane Science*, 2013, vol. 447, pp. 287-296. 10.1016/j.memsci.2013.07.026 . hal-00904294

**HAL Id: hal-00904294**

**<https://hal.science/hal-00904294>**

Submitted on 14 Nov 2013

**HAL** is a multi-disciplinary open access archive for the deposit and dissemination of scientific research documents, whether they are published or not. The documents may come from teaching and research institutions in France or abroad, or from public or private research centers.

L'archive ouverte pluridisciplinaire **HAL**, est destinée au dépôt et à la diffusion de documents scientifiques de niveau recherche, publiés ou non, émanant des établissements d'enseignement et de recherche français ou étrangers, des laboratoires publics ou privés.



## Open Archive TOULOUSE Archive Ouverte (OATAO)

OATAO is an open access repository that collects the work of Toulouse researchers and makes it freely available over the web where possible.

This is an author-deposited version published in : <http://oatao.univ-toulouse.fr/>  
Eprints ID : 9762

**To link to this book chapter** : DOI:10.1016/j.memsci.2013.07.026  
URL : <http://dx.doi.org/10.1016/j.memsci.2013.07.026>

**To cite this version** : Pellegrin, Bastien and Prulho, Romain and Rivaton, Agnès and Thérias, Sandrine and Gardette, Jean-Luc and Gaudichet-Maurin, Emmanuelle and Causserand, Christel. *Multi-scale analysis of hypochlorite induced PES/PVP ultrafiltration membranes degradation*. (2013) Journal of Membrane Science, vol. 447 . pp. 287-296. ISSN 0376-7388

Any correspondence concerning this service should be sent to the repository administrator: [staff-oatao@listes-diff.inp-toulouse.fr](mailto:staff-oatao@listes-diff.inp-toulouse.fr)

# Multi-scale analysis of hypochlorite induced PES/PVP ultrafiltration membranes degradation

Bastien Pellegrin<sup>a,b,1</sup>, Romain Prulho<sup>c,d,1</sup>, Agnès Rivaton<sup>c,d</sup>, Sandrine Thérias<sup>c,d</sup>, Jean-Luc Gardette<sup>c,d</sup>, Emmanuelle Gaudichet-Maurin<sup>e</sup>, Christel Causserand<sup>a,b,\*</sup>

<sup>a</sup> Université de Toulouse, INPT, UPS, Laboratoire de Génie Chimique, 118 route de Narbonne, F-31062 Toulouse cedex 09, France

<sup>b</sup> CNRS, UMR 5503, Laboratoire de Génie Chimique, F-31062 Toulouse, France

<sup>c</sup> Clermont Université, Université Blaise Pascal, ICCF, BP 10448, F-63000 Clermont-Ferrand, France

<sup>d</sup> CNRS, UMR 6505, ICCF, BP 80026, F-63171 Aubière, France

<sup>e</sup> Veolia Environnement Research and Innovation, Maisons-Laffitte Research Center, Chemin de la digue BP 76, 78603 Maisons-Laffitte cedex, France

## A B S T R A C T

In drinking water production plants, the use of oxidants such as sodium hypochlorite during in-place cleanings may impair the membrane integrity and radically impact the ultrafiltration process efficiency, leading to potential contamination of the permeate water with pathogens. This study investigates the effects of hypochlorite exposure on the properties of a commercially available UF hollow fiber. Mechanical performances and water permeability appeared to be greatly affected by the contact with hypochlorite. Monitoring the molecular changes by X-ray photoelectron spectroscopy (XPS), attenuated total reflectance infrared spectroscopy (ATR-IR), size exclusion chromatography (SEC) and VITA-mode atomic force microscopy (VITA-AFM) revealed high stability of the main polymer constituting the membrane (i.e. polyethersulfone (PES)) and very high reactivity of the additive (i.e. poly(N-vinyl pyrrolidone) (PVP)) towards immersion in aqueous sodium hypochlorite solution with maximal reaction rate for neutral to slightly basic pH. Correlation of those results unexpectedly leads to the conclusion that the overall membrane properties changes are governed by the additive fate.

## Keywords:

Ageing  
Hypochlorite cleaning  
PES  
PVP  
Ultrafiltration

## 1. Introduction

The use of hollow fiber ultrafiltration membranes is becoming an increasingly popular method for drinking water production. In order to avoid clogging and bacterial contamination, frequent in-place washings are necessary to clean membranes. Such cleaning can be achieved by backwashing and chemical cleaning procedures using hydrochloric acid, sodium hydroxide, and oxidants as hydrogen peroxide ( $H_2O_2$ ) or sodium hypochlorite (NaOCl). Sodium hypochlorite is by far the most commonly used cleaning reagent [1]. However, major water treatment facilities appear to be subjected to membrane failure and integrity loss on a quite regular basis, leading, in some cases, to failure frequency rates as high as one hollow fiber rupture per module and per year [2]. One can suspect, even if on-site data are not officially available, that membrane performances are affected before their rupture. It is then necessary to understand the mechanisms responsible for such a loss of integrity in order to be able to anticipate membrane

failure and to provide advices to drinking water producers concerning the cleaning conditions that should be applied or avoided.

The chemistry of aqueous NaOCl solutions is pH dependent. In water, sodium hypochlorite is totally dissociated, leading to the formation of hypochlorous acid (HClO) and sodium hydroxide (NaOH). Within the pH range (pH 6–11) commonly encountered during cleaning procedures, the weak acid HClO may then be deprotonated to its conjugate base, the hypochlorite ion ( $ClO^-$ ) with a  $pK_a$  value of 7.58 at 20 °C [3]. HClO species is known to be a much more effective disinfectant with a higher oxidizing power in comparison to  $ClO^-$  [4]. For those reasons, pH value of aqueous hypochlorite solution is of crucial importance regarding the cleaning efficiency and the membrane degradation phenomenon and has to be precisely investigated.

Commonly, PES based membranes are modified with polymeric additives such as poly(N-vinyl pyrrolidone) (PVP) in order to improve hydrophilicity and tune the membrane porous structure. Previous works have shown that sodium hypochlorite has a strong impact on the PVP additive [5–7] leading to an increase of pure water permeability.

PES is commonly considered as a polymer highly resistant to oxidants and tolerant to a wide range of pH (from 2 to 12). Wienk et al. reported for instance PES polymer stability when immersed in a 3000 ppm hypochlorite solution during 48 h under stirring [5,6]. However, a few authors investigated the impact of

\* Corresponding author at: Université de Toulouse, INPT, UPS, Laboratoire de Génie Chimique, 118 route de Narbonne, F-31062 Toulouse cedex 09, France. Tel.: +33 5 61 55 86 90; fax: +33 5 61 55 61 39.

E-mail addresses: [pellegrin@chimie.ups-tlse.fr](mailto:pellegrin@chimie.ups-tlse.fr) (B. Pellegrin), [caussera@chimie.ups-tlse.fr](mailto:caussera@chimie.ups-tlse.fr) (C. Causserand).

<sup>1</sup> These authors contributed equally to this work.

sodium hypochlorite on PES membranes and proposed a chain scission phenomenon at the ether–sulfone linkage [8–10]. Thominet et al. [8] reported chain scission of PES and an alteration of hollow fiber membranes mechanical properties when exposed to a 400 ppm hypochlorite solution at pH 8 for up to 120 days (1,152,000 ppm h) at room temperature. Similarly, Arkhangelsky et al. [9] studied the impact of hypochlorite exposure (up to 100,000 ppm h–150 ppm at pH 7.2 for up to 28 days at room temperature) on commercial PES flat sheet membranes containing PVP additive. They reported an increase of the pure water permeability and a decrease of the mechanical properties of the membranes attributed to both PES and PVP degradation. Subsequently, Yadav et al. [11,12] investigated PES composite membrane samples soaked in 700 ppm hypochlorite solutions for up to 36 days (up to 600,000 ppm h) at 55 °C for both pH 9 and 12. They observed by ATR-IR the outbreak of a new band at 1034 cm<sup>-1</sup> and assigned it to the formation of sulfonic acid due to the degradation of the PES layer. On the basis of a PES degradation mechanism suggested by Thominet et al. [8] and Arkhangelsky et al. [9] they then proposed a degradation mechanism including chain scissions of the PES and formation of sulfonic acid and phenyl chloride and groups. In the present work, specific experiments and characterizations were designed and used to go further in the understanding of the molecular mechanisms of degradation induced by hypochlorite on PES/PVP hollow fibers membranes.

In this aim, PES/PVP fibers were put in contact with a bleach solution at various pH values, increasing doses (concentration x exposure time) and constant temperature 20 ± 2 °C. As it is well known that in most cases the deterioration of the macroscopic properties of polymers results from modifications of their chemical structure [13], the goal of this study was to elucidate the degradation mechanisms of the fiber at the molecular level and to correlate those modifications with the macroscopic properties. In this work, the term ageing refers to the modification of the membrane properties. Since no direct correlation between laboratory ageing and ageing actually happening during regular on-site operation (on-site ageing) has been established yet, the term accelerated ageing is avoided. Consequently, the other objective is to validate the laboratory ageing protocols representativeness regarding the molecular scale degradation mechanisms and the impact on the macroscopic performances as compared to the actual on-site ageing phenomenon.

Fibers have been analyzed with several techniques allowing different levels of analysis. At molecular scale: X-ray photoelectron spectroscopy (XPS) and attenuated total reflectance infrared spectroscopy (ATR-IR) were used to understand the changes of functional groups, allowing therefore to elucidate the degradation mechanisms. At supramolecular scale: size exclusion chromatography (SEC) and VITA-mode atomic force microscopy (VITA-AFM) allowed us to monitor the extent of chain scissions. Finally, regarding macroscopic properties: tensile testing was performed to investigate the mechanical properties, pure water permeability was monitored and morphological changes were observed by scanning electron microscopy (SEM). Evaluation of the depth profile of the degradation was also carried out thanks to a micrometric profilometer. This multi-scale characterization allowed us to propose a degradation mechanism of PES/PVP hollow fibers that has been validated on PES/PVP dense films and published in former work [14] and to correlate it to the evolution of the fibers operating performances.

In previous studies [15], it has been suggested that hydroxyl radicals could be responsible for the degradation of polysulfone membranes in contact with hypochlorite cleaning solutions. Particular efforts have been deployed in the present study to investigate the role of free radicals in the case of hypochlorite induced degradation of PES/PVP membrane.

## 2. Material and methods

### 2.1. Membranes

The membranes used in this study are commercially available hollow fibers extracted from a new UF module (HYDRACAP 60, LD HYDRANAUTICS Membrane), widely used for drinking water production. Those hollow fibers present an asymmetric geometry with an inner selective layer, an internal diameter of 0.8 mm and an external diameter of 1.3 mm (Fig. 1a). Manufacturer datasheet also specifies a molecular weight cut-off (MWCO) of 150 kDa, a maximum operating trans-membrane pressure (TMP) of 1.4 bar (0.14 MPa) and a maximum chlorine exposure of 200,000 ppm h (200 g h L<sup>-1</sup>). Membrane material is claimed to be a “hydrophilized” PES (Fig. 1b). As described in Section 3.2.1, the additive used for the membrane surface hydrophilization has been identified by ATR-IR to be PVP (Fig. 1c), and typically accounts for up to 5–10 wt% of the final membrane material.

After extraction from the module, the hollow fibers were stored in a 1 g L<sup>-1</sup> sodium bisulfite (Na<sub>2</sub>O<sub>4</sub>S<sub>2</sub> – Technical grade 85%, Sigma-Aldrich, USA) solution at 5 °C to avoid bacterial proliferation. Prior to using, membrane samples were soaked in a large volume of ultra-pure water for a minimum time of 1 h to remove sodium bisulfite.

### 2.2. Solutions and chemicals

All aqueous solutions were prepared using deionized ultrapure water ( $\rho$ =18.2 MΩ cm) generated by a PURELAB Maxima system

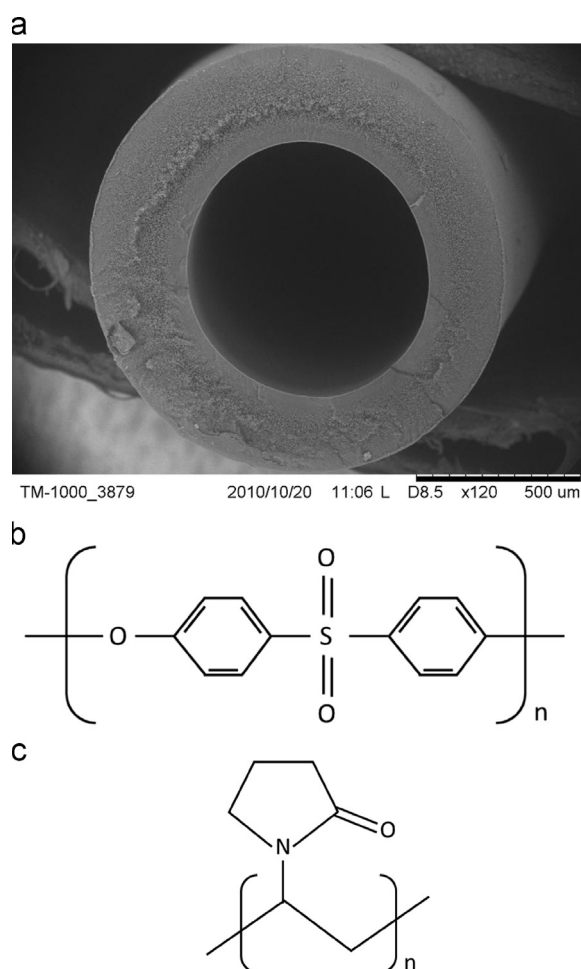


**Fig. 1.** Cross-section SEM image of a nitrogen-fractured pristine membrane (a); molecular structure of polyethersulfone (b) and poly(N-vinyl pyrrolidone) (c).



(ELGA LabWater's, UK). Hypochlorite solutions used for the ageing experiments were obtained by dilution of a commercial NaOCl reagent (NaOCl 9.8 wt% – La Croix, Fr). Concentrated sulfuric acid ( $\text{H}_2\text{SO}_4$  – Analytical grade 95%, VWR PROLABO, Fr) and sodium hydroxide (NaOH – Analytical grade, CARLO ERBA Reagents, Fr) were added to the hypochlorite ageing solutions to adjust their pH value.

Some ageing experiments were performed with the addition of a radical scavenger to the hypochlorite solution. For this purpose, the 2-methylpropan-2-ol ( $t\text{BuOH}$  – HPLC grade 99.5%, SIGMA-ALDRICH, USA) was selected for its high reactivity towards hydroxyl free radicals ( $\text{HO}^\bullet$ ).

SEC characterization of the membrane material required to dissolve membrane samples in an effective solvent.  $N,N$ -dimethylmethanamide (DMF – Analytical grade, CARLO ERBA Reagents, Fr) was used as a solvent and as an eluent for membrane dissolutions and the SEC measurements.

## 2.3. Ageing protocols

### 2.3.1. Sodium hypochlorite treatment

Ageing experiments were all performed by soaking the membranes at ambient temperature ( $20 \pm 2^\circ\text{C}$ ) in hypochlorite solutions at a total free chlorine concentration ([TFC]) of 350 ppm ( $\text{mg L}^{-1}$ ). Exposure times ranged from 1 h to 28 days. [TFC] was monitored using the so called DPD method (EPA-approved method 4500 Cl G): reaction of chlorine-containing samples with  $N,N$ -diethyl- $p$ -phenylenediamine sulfate in the presence of a specific buffer producing a pink colored compound, measured at 520 nm using a spectrophotometer (DR/2400, HACH, USA). The pH of the soaking solutions ranging from 6 to 11 was then adjusted by addition of  $\text{H}_2\text{SO}_4$  and NaOH. Since pH 8 and 11 values approximately correspond to onsite back-washing and chemical cleaning pH conditions respectively, they were more extensively investigated. In addition, pH 6 was also studied in more detail, since it corresponds to the prevalence of  $\text{HClO}$  species, whereas pH 11 corresponds to  $\text{ClO}^-$  species predominance and pH 8 leads to the coexistence of both  $\text{HClO}$  and  $\text{ClO}^-$  species (Fig. 2). Since [TFC] and pH were found to be decreasing with time, constant [TFC] ( $\pm 30$  ppm) and pH ( $\pm 0.2$ ) were maintained by daily adjustment of the soaking solutions.

Membrane control samples were similarly soaked in ultra-pure water up to 28 days. Another set of NaOCl ageing experiments was performed using the conditions mentioned above with the addition of  $2 \text{ g L}^{-1}$  of  $t\text{BuOH}$  as a radical scavenger in the soaking solution.

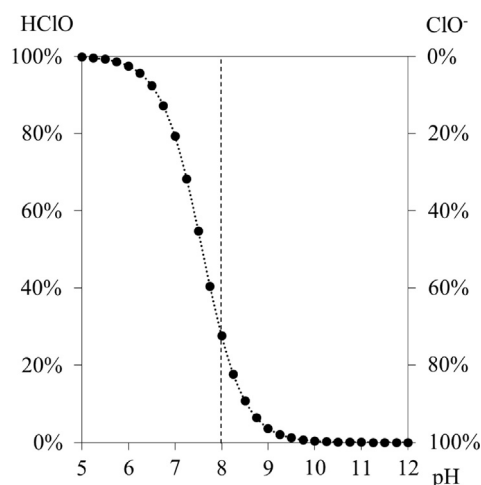


Fig. 2.  $\text{HClO}$  and  $\text{ClO}^-$  species dissociation curve at  $20^\circ\text{C}$ , obtained by calculation, using  $\text{pK}_a(\text{HClO}/\text{ClO}^-) = 7.58$  at  $20^\circ\text{C}$  [3].

After each ageing experiment, samples were soaked in a large volume of ultra-pure water for 2 h and stored in a  $1 \text{ g L}^{-1}$   $\text{Na}_2\text{O}_4\text{S}_2$  solution at  $5^\circ\text{C}$  for later analysis.

Usually, for on-site operation, membranes are periodically subjected to free chlorine contact during back-washing and chemical cleaning. Depending on the characteristics of the treated water, water treatment facilities operators may use NaOCl solutions with a [TFC] up to 20 ppm during up to 5 min for back-washing process and with a [TFC] up to 400 ppm for up to 2 h for chemical cleaning process. Frequency may reach, for back-washing and chemical cleaning respectively, 1/6 h of membrane operation and 1/month of membrane operation. Even if membranes are only periodically in contact with hypochlorite, the combined amount of NaOCl in contact with membranes can be expressed as a total dose. Hypochlorite dose will then refer to the [TFC] of the NaOCl soaking solution, multiplied by the sample NaOCl exposure time. For convenience, NaOCl dose will be expressed in  $\text{g h L}^{-1}$  ( $1000 \text{ ppm h}$ ) in the subsequent paragraphs, which is the most appropriate unit for the range of doses studied. Increasing the [TFC] and reducing the total exposure time can be a direct way to perform accelerated ageing experiments and to predict the impact of hypochlorite on membranes during on-site operation, but this trivial factorization is not entirely above criticism. Additional soaking experiments were performed at various [TFC] to assay the validity of this concept.

Additionally, similar PES/PVP membranes extracted from a module operated on a French water production plant were collected and analyzed. Comparison with the laboratory aged samples was carried out.

### 2.3.2. Thermo-oxidation experiments

Thermo-oxidation experiments on pristine membranes were performed in a ventilated oven at  $100^\circ\text{C}$  over 60 days.

## 2.4. Membrane characterization

### 2.4.1. Permeability measurements

Pure water permeability of pristine and hypochlorite aged membrane samples was quantified with a cross-flow filtration set-up at controlled temperature of  $20 \pm 5^\circ\text{C}$ . Ultra-pure water was forced to permeate from the inside to the outside of a 15 hollow fibers laboratory scale module ( $220 \pm 5 \text{ mm}$  length). The trans-membrane pressure (TMP) was applied by adjusting a pressure valve at the retentate side. To overcome the impact of membrane compaction, each module tested was first subjected to cross-flow filtration of ultra-pure water at maximal TMP of 0.14 MPa until pure water flux stabilization (20 min). After membrane compaction, the TMP ranged from 0.05 to 0.14 MPa and taken as the average of the feed pressure and the retentate side pressure readings, upstream of the pressure valve. The pure water permeability at  $20^\circ\text{C}$  ( $L_p/\mu_{20}$  in  $\text{L h}^{-1} \text{ m}^{-2} \text{ bar}^{-1}$ , with  $L_p$  the permeability coefficient and  $\mu_{20}$  the water viscosity at  $20^\circ\text{C}$ ) was then calculated, as described in former work [16], from the Darcy law:

$$J_T = \frac{L_p}{\mu_T} \Delta P \quad (1)$$

where  $J_T$  is the permeate flux density ( $\text{L h}^{-1} \text{ m}^{-2}$ ) calculated using the inner surface area of the membranes and  $\mu_T$  the fluid viscosity for the experiment temperature.

The flux density  $J_T$  was corrected back to  $J_{20}$  using the empirical Arrhenius law of the fluid viscosity variation as a function of the temperature.

$$J_{20} = J_T \frac{\mu_T}{\mu_{20}} = J_T \exp\left(\frac{E_0}{RT} - \frac{E_0}{293R}\right) \quad (2)$$

where  $E_0$  is the activation energy of the fluid (for water  $E_0=15\,675\text{ J mol}^{-1}$ ),  $R$  the universal gas constant and  $T$  the temperature of the experiment.

$L_p/\mu_{20}$  was then taken as the slope value of the linear regression between  $\Delta P$  and  $J_{20}$  values.

#### 2.4.2. Scanning electron microscopy (SEM)

SEM images of the cross-section of membranes were recorded using a HITACHI Tabletop Microscope TM-1000. Prior to analysis, membrane samples were fractured in liquid nitrogen, dried in a vacuum oven at room temperature for 1 h and coated with a 5 nm silver layer. To obtain an accurate representation of membrane cross-section morphology, a set of 6–10 images was recorded for each condition investigated. Image editing and treatment were performed using IMAGEJ<sup>®</sup> software.

#### 2.4.3. Tensile strain at break measurements

Tensile tests were performed on wet membranes using an INSTRON 3342 series tensile apparatus. Tailor-made grips for the hollow fiber geometry were fitted to the device to avoid stress concentration. Initial distance between grips was fixed to 110 mm and samples were extended at a constant elongation rate of  $100\text{ mm min}^{-1}$ . Young's modulus  $E$ , tensile stress at break  $\sigma_R$  and elongation at break  $\epsilon_R$  were calculated from the experimental stress–strain curves. A set of eight samples was analyzed and averaged for each condition analyzed.

#### 2.4.4. Attenuated total reflection-Fourier transform infrared (ATR-IR) spectroscopy

Infrared spectra of the inner active layer of membranes were recorded using a THERMO-NICOLET Nexus 670 fitted with a DTGS detector and a diamond ATR crystal. Spectra were obtained by summation of 16 scans between  $4000$  and  $400\text{ cm}^{-1}$  with a resolution of  $4\text{ cm}^{-1}$ . Spectral analysis was performed on OMNIC<sup>®</sup> software. Membrane samples were axially cut open to gain access to the inner active layer for analysis. Prior to analysis, samples were dried in a vacuum oven for 2 h at  $50\text{ }^\circ\text{C}$  and shortly stored in a desiccator. All the IR spectra recorded were corrected by adjusting the  $1150\text{ cm}^{-1}$  band (which corresponds to  $\text{SO}_2$  symmetric stretching of PES and considered to be invariant during the membrane degradation) to an arbitrary chosen absorbance value of 1. In the subsequent paragraphs, the corrected absorbance is mentioned as relative absorbance. To facilitate the reader's understanding, when monitoring changes of specific IR bands upon degradation, normalization back to the pristine membrane relative absorbance may be performed. Likewise, when carrying out profile analysis, normalization back to the surface value may be performed.

Note that ATR-IR technique generates a few microns depth penetration of the infrared beam in the sample thickness; therefore it is commonly considered that infrared spectrum obtained using a diamond ATR crystal provides information regarding the first  $3\text{--}5\text{ }\mu\text{m}$  underneath the membrane surface. All absorbance values presented are an average of at least four samples.

In addition, ATR-IR profiles of the membrane section were performed. To gain access to the membrane bulk, successive mechanical abrasions from the membrane surface were carried out with a BUEHLER ISOMET 5000 precision saw. ATR-IR spectra were then recorded for each abrasion depth according to the aforementioned protocol.

#### 2.4.5. X-ray photoelectron spectroscopy (XPS)

XPS analyses of the inner active layer of membranes were performed using an Escalab 250 (THERMO ELECTRON) device with  $\text{Al K}\alpha$  radiation as the X-ray monochromatic source ( $1486.6\text{ eV}$ ). Unlike

ATR-IR, XPS technique allows chemical characterization of sample surfaces, with an analysis depth in the nanometer range. XPS measurements were repeated on three distinct samples for each condition analyzed. Prior to active layer analysis, membrane samples were dried and axially cut open to gain access to the inner surface.

#### 2.4.6. Size exclusion chromatography (SEC)

SEC chromatograms of membrane material dissolved in DMF at a concentration of  $5\text{ g L}^{-1}$  were performed using a refractometer fitted apparatus connected to two TOSOH BIOSCIENCE columns (TSK-Gel Alpha 3000 and 5000). Analyses were performed at a flow rate of  $1\text{ mL min}^{-1}$  and the detector was calibrated with polyethylene glycol standards. DMF was used as the eluent. The peak corresponding to the elution time of PES was then analyzed to obtain the molecular mass distribution of PES.

#### 2.4.7. Nanoscale thermal analysis module (VITA)

The changes of the glass transition temperature ( $T_g$ ) of the polymers constituting the membrane were followed at the extreme surface of the membrane using an AFM nanoscale thermal analysis module (VITA). This technique allows the determination of the local glass transition temperature of polymers with a nanoscale spatial resolution. The probe temperature increase causes a progressive thermal expansion of the polymer, which leads to a cantilever deflection. When the probe temperature reaches a transition temperature of the polymer (such as the  $T_g$ ), the probe penetrates into the sample. This penetration causes an opposite deflection that can be detected by the AFM. Temperature recorded for an inverted probe deflection will then correspond to a local  $T_g$ . The specific probes used for this type of measurements are comprised of an electric circuit connected to the Vita module. The temperature of the probe is increased by applying an electric current to this circuit (Joule effect). A relation between the probe temperature and the applied tension can be established by calibrating the probe with several known polymers. The spring constant of the probe was chosen between  $0.5\text{ N m}^{-1}$  and  $3\text{ N m}^{-1}$ , and its cantilever was  $200\text{ mm}$  long. The probe was calibrated using three standard polymers: polycaprolactone ( $T_m=55\text{ }^\circ\text{C}$ ), polyethylene ( $T_m=116\text{ }^\circ\text{C}$ ) and polyethylene terephthalate ( $T_m=235\text{ }^\circ\text{C}$ ).

Measurements were performed on pristine and aged membranes to investigate potential changes in the thermal properties of the samples during the degradation. Each measurement was performed five times to ensure good reproducibility. During these experiments, the probe was heated from  $45\text{ }^\circ\text{C}$  to  $230\text{ }^\circ\text{C}$  at a heating rate of  $10\text{ }^\circ\text{C s}^{-1}$ .

### 3. Results and discussion

#### 3.1. Macroscopic characterization

The impact of hypochlorite exposure on the global mechanical performances of the hollow fibers was investigated by tensile testing. Fig. 3 presents typical shapes of stress–strain curves obtained for pristine and hypochlorite treated membranes. The virgin membranes exhibited a Young's modulus  $E$  of  $80 \pm 6\text{ N mm}^{-2}$ , a tensile stress at break  $\sigma_R$  of  $5.0 \pm 0.3\text{ MPa}$  and an elongation at break  $\epsilon_R$  of  $57 \pm 4\%$ . After exposure to hypochlorite, the overall envelope of the stress–strain curves remained mostly unchanged in the elastic domain and in the early stages of the plastic domain, while the elongation at break  $\epsilon_R$  value appeared to be largely affected. That is to say, during tensile testing, sample fracture occurred sooner as the hypochlorite dose was increased. Therefore, choice was made to monitor the changes of  $\epsilon_R$  since it was found to be the most sensitive parameter.

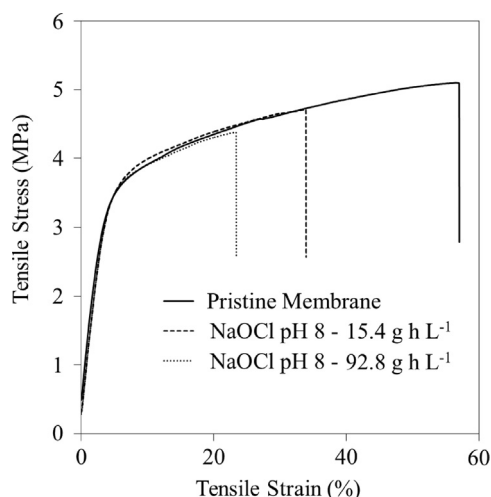


**Fig. 3.** Examples of tensile stress-strain curves of pristine membrane and membranes exposed to hypochlorite doses of  $15.4 \text{ g h L}^{-1}$  (350 ppm – 44 h) and  $92.8 \text{ g h L}^{-1}$  (350 ppm – 265 h) at pH 8.

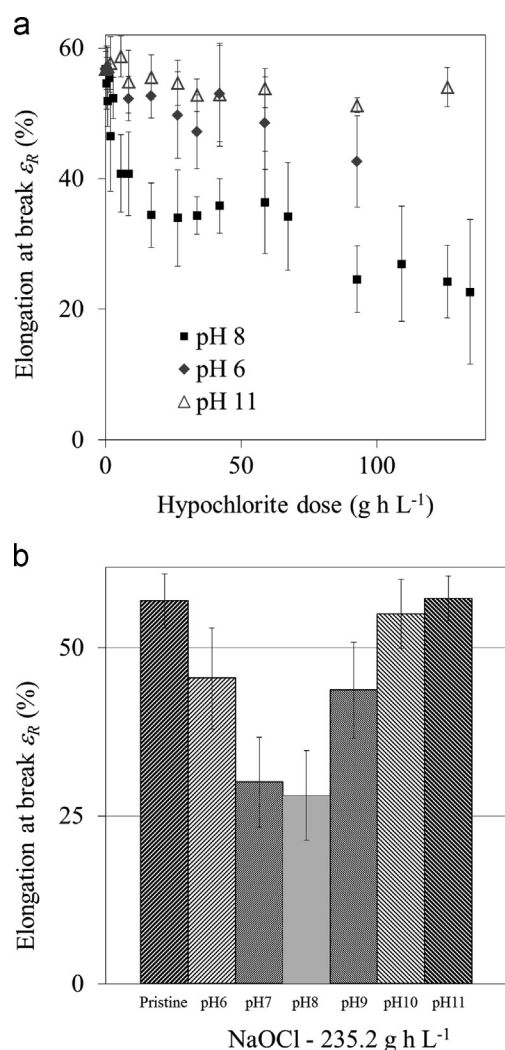


**Fig. 4.** Elongation at break  $\epsilon_R$  of membranes exposed to various doses of sodium hypochlorite at pH 6, 8 and 11 (a); elongation at break  $\epsilon_R$  of membranes exposed to hypochlorite at a dose of  $235.2 \text{ g h L}^{-1}$  (350 ppm – 672 h) at various pH values (b).

The  $\epsilon_R$  values obtained for a wide range of soaking conditions (various hypochlorite exposure time and pH) are reported in Fig. 4a. Decrease of the elongation at break  $\epsilon_R$  of membranes arose from contact with hypochlorite solution, meaning that membrane ductility decreased for aged samples. Same observations were already made by several authors [8,10,11] that all reported PES membranes mechanical properties severely affected by hypochlorite exposure. The  $\epsilon_R$  drop was the most significant for the experiment conducted at pH 8. A few authors also reported the incidence of pH regarding membrane embrittlement rate when exposed to hypochlorite solution.

Fig. 4b presents the results obtained for membrane elongation at break  $\epsilon_R$  as a function of the pH value of the soaking solution (ranging from 6 to 11) for a hypochlorite dose of  $235.2 \text{ g h L}^{-1}$  (350 ppm – 672 h), just above the  $200 \text{ g h L}^{-1}$  maximum chlorine exposure recommended by the manufacturer. It clearly appears that the most significant  $\epsilon_R$  decrease was undergone by membranes exposed to pH 7 and pH 8 solutions. In other words, the embrittlement of aged membranes strongly depends on the pH of the hypochlorite solution and the closer we get from pH 7 to pH 8 range, the more severe the ductility loss will be. A few authors [11,15,17] also reported the incidence of pH regarding membrane embrittlement rate when exposed to hypochlorite solution. For instance, Yadav et al. [11] similarly reported higher impact on membrane mechanical performances when exposed to hypochlorite solution at pH 9 than at pH 12. Furthermore, according to Fig. 4a and b, for very high hypochlorite doses,  $\epsilon_R$  value reaches a relative stabilization at  $25 \pm 10\%$  for pH 8 aged membranes.

Impact of hypochlorite in terms of water transfer through the membrane is shown in Fig. 5a, where the membrane pure water permeability  $L_p/\mu_{20}$  is reported as a function of the hypochlorite dose and the pH value of the soaking solution. For pH 6, 8 and 11, contact with low doses of hypochlorite induced a drastic increase of  $L_p/\mu_{20}$ . Besides, for early stages of the degradation and at equivalent hypochlorite dose, the  $L_p/\mu_{20}$  increase was more substantial for pH 8 than for pH 6 and 11. For higher hypochlorite doses, this difference tended to lessen and  $L_p/\mu_{20}$  reached a quasi-stabilization for all pH values studied.

Fig. 5b reports the permeability values of membranes exposed to the same hypochlorite dose of  $235.2 \text{ g h L}^{-1}$  (350 ppm – 672 h), at pH values ranging from 6 to 11. At this high hypochlorite dose and for all pH values studied,  $L_p/\mu_{20}$  increased to the same extent, reaching 1.9–2.2 times the initial  $L_p/\mu_{20}$  value. As a conclusion, prolonged contact with hypochlorite induced a pronounced gain in water transfer through the membrane, but, unlike the results regarding the mechanical properties, the permeability increase did not show clear dependency on the pH of the soaking solutions. Arkhangelsky et al. [9] and Yadav et al. [12] similarly reported a pure water permeability increase for PES and PES/PVP UF membranes and Rouaix et al. [17] reported a comparable increase on PSf/PVP membranes.

Changes of the membrane structure were also monitored by SEM imaging of the membrane cross-section. Fig. 1a presents an example of an image recorded at a magnification of  $120 \times$ . A whole set of images were performed on new and severely aged ( $235.2 \text{ g h L}^{-1}$ , pH 8) membrane cross-sections and internal surface (not shown here). Even at higher magnification (up to  $10,000 \times$ ), SEM imaging failed to detect any noticeable changes regarding the membrane macroporous structure and surface aspect unlike several authors that observed surface cracking and pitting [10,11].

### 3.2. Molecular and supramolecular characterizations

Majority of the experiments reported in this section has been obtained with membrane samples soaked in hypochlorite solution at pH 8 since, according to previous results, this pH corresponds to



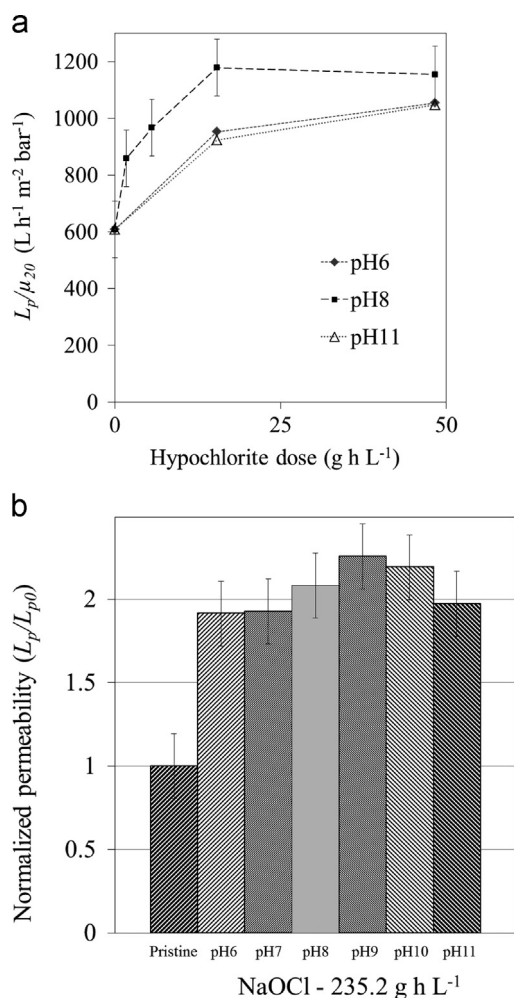


**Fig. 5.** Permeability of membranes exposed to various doses of sodium hypochlorite at pH 6, 8 and 11(a); normalized permeability of membranes exposed to hypochlorite at a dose of  $235.2 \text{ g h L}^{-1}$  (350 ppm – 672 h) at various pH values (b).

the most severe modification in membrane mechanical properties and permeability.

### 3.2.1. PES and PVP degradation products identification

The ATR-IR spectra of pristine membrane and of membranes treated with a hypochlorite dose of  $235.2 \text{ g h L}^{-1}$  (350 ppm – 672 h) at pH 8 are shown in Fig. 6. The intensity of the IR band at  $1674 \text{ cm}^{-1}$  attributed to the stretching vibration of the amide unit of the PVP [18], is lower in the hypochlorite-treated membrane than in the pristine one, which indicates either a degradation of the PVP or a decrease in PVP content in the first microns of the membrane surface.

This decrease comes with the appearance of four new bands: three bands at  $1540 \text{ cm}^{-1}$ ,  $1700 \text{ cm}^{-1}$  and  $1770 \text{ cm}^{-1}$  ascribed to PVP degradation products and the last one, at  $1034 \text{ cm}^{-1}$ , attributed to PES oxidation. Oxidation products of PVP were identified as succinimide ( $1700/1770 \text{ cm}^{-1}$ ) and a secondary amide ( $1540 \text{ cm}^{-1}$ ) [14]. Yadav et al. [11] similarly observed the appearance of a  $1034 \text{ cm}^{-1}$  band and they ascribed it to a sulfonic acid resulting from the PES chain scission mechanism they proposed. In already published study, proof was made that this band does not correspond to a sulfonic acid and the IR band at  $1034 \text{ cm}^{-1}$  was shown to reveal the formation of an ortho-substituted phenol on the PES backbone [14]. No other changes on the characteristic

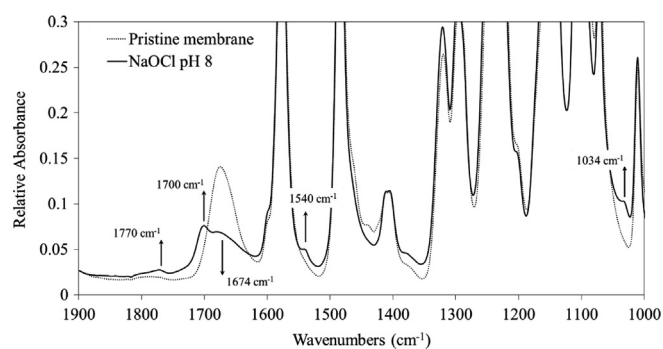


**Fig. 6.** ATR-FTIR spectra of the intern surface of a pristine membrane and an aged membrane ( $235.2 \text{ g h L}^{-1}$  at pH 8).

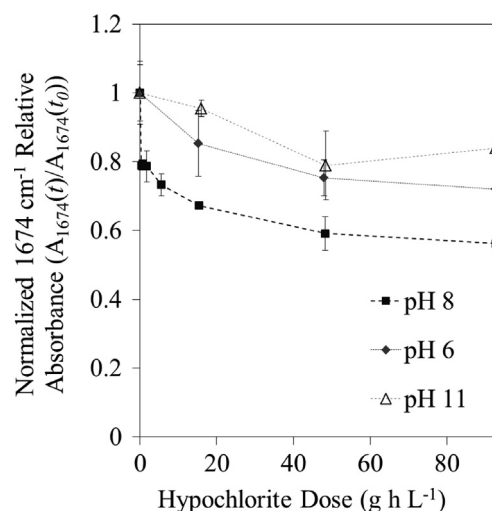


**Fig. 7.** Normalized relative IR absorbance of the  $1674 \text{ cm}^{-1}$  band measured on membranes exposed to various doses of sodium hypochlorite at pH 6, 8 and 11.

bands of PES were detected. Those spectra changes contradict the observations made by Arkhangelsky et al. that reported no appearance of new bands, an unchanged PVP amide unit band and a decrease of the  $1485 \text{ cm}^{-1}$  band [9].

The impact of the hypochlorite solution pH value on the decrease of the IR band of PVP was also investigated. Fig. 7 presents the PVP band ( $1674 \text{ cm}^{-1}$ ) relative absorbance, normalized back to the initial value of the pristine membrane ( $A_{1674}(t)/A_{1674}(t_0)$ ) as a function of the hypochlorite dose. Results are reported for pH 6, 8 and 11. For all pH values studied, the normalized relative absorbance of the PVP band decreased for increasing hypochlorite dose. The PVP band intensity decrease was prompter and more significant for pH 8 than for pH 6 and 11.

XPS measurements were also conducted to investigate the chemical composition of the membrane surface upon hypochlorite treatment. Results in terms of elemental concentration obtained for pristine and  $84 \text{ g h L}^{-1}$ , pH 8 treated membranes are reported in former work [16]. Since PES and PVP monomer units respectively carry only one sulfur atom (S) and one nitrogen atom (N), the N/S atomic ratio is a direct evaluation of the fraction of PVP present on the membrane surface. The N/S atomic ratios were 0.44 for the pristine membrane and 0.30 for the  $84 \text{ g h L}^{-1}$ , pH 8 treated membrane. Using the molar weight of PES and PVP monomers ( $232 \text{ g mol}^{-1}$  and  $110 \text{ g mol}^{-1}$  respectively), it can be calculated that PVP accounts for 17.1 wt% on the pristine membrane surface and 12.3 wt% on the aged membrane surface. Those results demonstrate that hypochlorite exposure does not only induce PVP degradation as shown by the appearance of new IR bands, but it also affects the PVP content of the membrane. Since no modification of the IR spectra and the N/S atomic

ratio was observed after soaking in water; conclusion can be made that the PVP degradation leads to its release from the membrane. Consequently, the decrease of the  $1674\text{ cm}^{-1}$  IR band can be imputed to both degradation and loss of PVP within the membrane material.

### 3.2.2. Molecular analysis within the membrane thickness

The changes of the  $1674\text{ cm}^{-1}$  band intensity were studied over the thickness of the membrane in order to quantify the initial PVP content within the pristine membrane structure and to correlate it to the PVP oxidation/release for the aged samples.

Fig. 8 presents, for pristine and hypochlorite treated membranes, the normalized PVP band relative absorbance as a function of the distance ( $d$ ) from the membrane internal surface ( $d_0$ ). For both the pristine and the aged membranes, the normalization of the  $1674\text{ cm}^{-1}$  band relative absorbance was calculated using the band relative absorbance of the pristine membrane, before abrasion ( $A_{1674}(d)/A_{1674}(d_0)$ ). Presence of PVP was significantly detected only within the first  $30\text{ }\mu\text{m}$  of the membrane thickness and contact with hypochlorite causes the PVP band to decrease. Additionally, Fig. 7 reports gray values obtained from processing of a membrane cross-section SEM image (presented in the lower part of the figure). The cross-section SEM image of the pristine membrane was binarized using arbitrary chosen thresholds. IMAGEJ software was then used to plot the gray value graph: the y-axis representing the averaged intensities of pixels along a vertical line within the binarized image and the x-axis representing the distance of the vertical line from the left side of the image.

We define here a structure presenting large voids or pores (larger than  $1\text{ }\mu\text{m}$ ) easily detectable by SEM imaging as macroporous. The gray value plot is then used as a macroporosity indicator: high and low gray values will respectively correspond to a macroporous and a denser material. It was found that PVP presence precisely coincides with the non-macroporous portion of the membrane cross-section. Note that the same type of observations can be made regarding the external part of the membrane

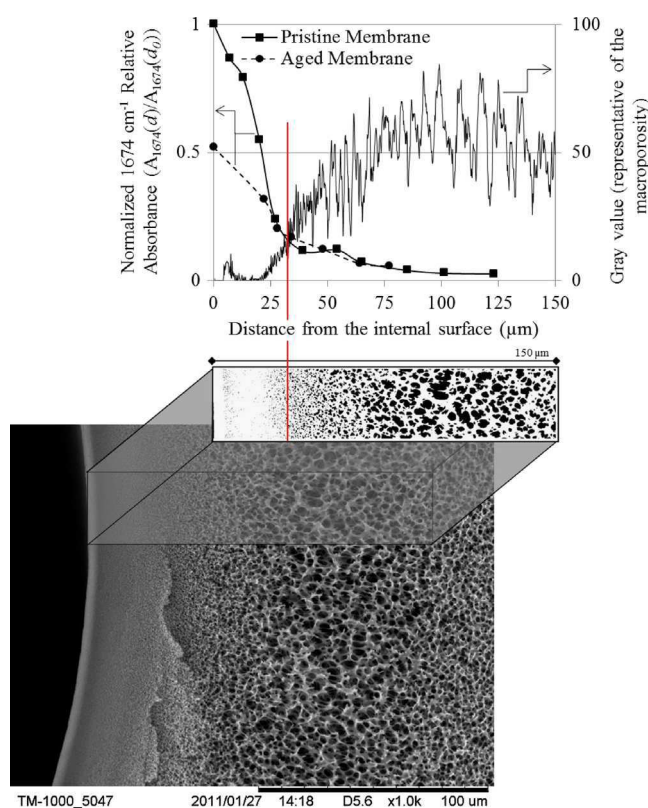


Fig. 8. PVP profile analysis on membrane thickness ( $1674\text{ cm}^{-1}$  band) on pristine and aged ( $235.2\text{ g h L}^{-1}$  at pH 8) membrane samples.

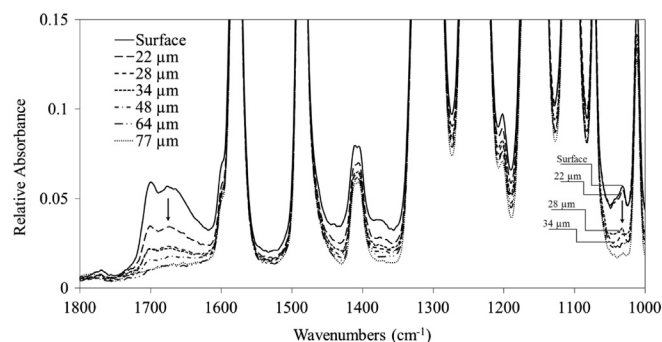


Fig. 9. ATR-IR profile analysis from the internal surface to a thickness of  $77\text{ }\mu\text{m}$  on a membrane treated with  $235.2\text{ g h L}^{-1}$  NaOCl at pH 8.

cross-section which also presents a relatively dense structure containing PVP (results not shown).

The ATR-IR spectra obtained from the internal surface to a thickness of  $77\text{ }\mu\text{m}$  on an aged membrane are reported in Fig. 9. It can be observed that the  $1034\text{ cm}^{-1}$  band, corresponding to the PES oxidation was only present for thickness values where the PVP ( $1674\text{ cm}^{-1}$ ) and PVP degradation products ( $1700/1770\text{ cm}^{-1}$ ) are present (i.e. approximately  $30\text{--}40\text{ }\mu\text{m}$ ). This observation demonstrates that the presence of PVP and/or PVP degradation products is a required condition for PES oxidation to occur.

### 3.2.3. Impact of membrane degradation at supramolecular scale

Modification of the molar weight distribution of the membrane polymers was characterized by SEC. Measurements were carried out on pristine and aged membrane materials dissolved in DMF. Chromatograms exhibited a monomodal distribution, PVP was then assumed to be in too small concentration in the overall membrane material to be detected by SEC. The average molar weight ( $M_w$ ) and the polydispersity index ( $M_w/M_n$ ) obtained for new and hypochlorite treated membranes were reported in former work [16]. Even at high dose ( $235.2\text{ g h L}^{-1}$ ) and at pH 8, hypochlorite exposure did not show any significant impact on the  $M_w$  and  $M_n$  of the PES with a constant  $M_w$  of  $40,200 \pm 2200\text{ g mol}^{-1}$  and a  $M_w/M_n$  of  $2.55 \pm 0.1$ . Former work has shown a significant decrease of  $M_w$  of hypochlorite exposed polysulfone (PSf) membranes [17]. PES appears to be more stable as compared to PSf when exposed to hypochlorite. This result was explained by the presence of a labile hydrogen in the PSf structure [14].

To study the impact of hypochlorite exposure on the PVP moieties at the very surface of the membranes, we used the AFM with nanoscale thermal analysis module. This Vita-mode allows us to determine the deflection temperature corresponding to the glass temperature ( $T_g$ ) of the polymer at the very surface of the membrane. The Vita-analysis was combined with depth abrasion to study the evolution of the  $T_g$  of the polymer within the thickness of the membrane (from the inner layer to the outer layer). Results are reported in Fig. 10.

Curves reported in Fig. 10 show the evolution of the glass transition of the polymer as a function of the distance from the internal surface of pristine and aged membranes. At the very surface of the pristine membrane, the  $T_g$  is  $165\text{ }^\circ\text{C}$  which is in the range of the  $T_g$  values commonly reported for PVP [19–21]. By monitoring the  $T_g$  from the inner surface to the membrane bulk, an increase of  $T_g$  is observed till reaching  $200\text{ }^\circ\text{C}$  (corresponding to the PES  $T_g$  [22–24]) at a distance of  $40\text{ }\mu\text{m}$  from the inner surface. The first  $40\text{ }\mu\text{m}$  membrane layer corresponds to high density area of the membrane with high PVP concentration. Same analysis was performed on membranes submitted to hypochlorite exposure ( $235.2\text{ g h L}^{-1}$ , pH 8). Ageing provoked an important decrease of  $T_g$



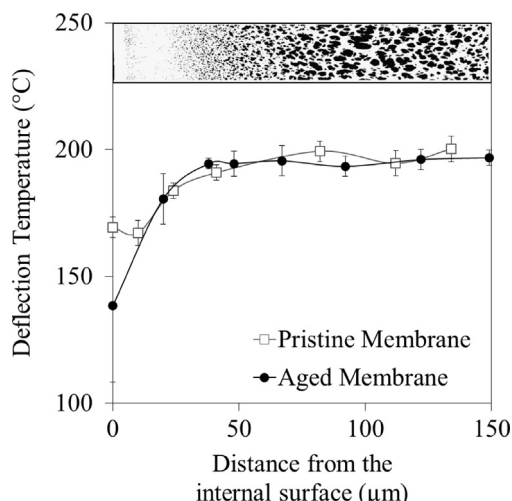


**Fig. 10.** Evolution of the deflection temperature ( $T_g$ ) as a function of the distance from the internal surface of pristine and aged membranes ( $235.2 \text{ g h L}^{-1}$ , pH 8).

at the very surface of the membrane from  $165^\circ\text{C}$  to  $138^\circ\text{C}$ ; this decrease goes along with a significant increase of the standard deviation due to the high degradation of the membrane surface. After ageing, no modification of the  $T_g$  in the membrane bulk was observed, meaning that no chain scission occurred in the membrane part exempt of PVP. The decrease of the  $T_g$  is a direct proof that the degradation of the membrane involves chain scissions of the PVP moieties. Chain-scissions in PVP are anticipated to weaken the structure and contribute to the loss of mechanical properties of the membrane.

#### 3.2.4. Identification of the active species: $\text{OH}^\bullet$ radicals

The ATR-FTIR spectra of pristine membrane and of membranes treated by thermo-oxidation according to the protocol presented in Section 2.3 are shown in Fig. 11. This type of treatment leads to ageing of polymer by oxidation involving  $\text{HO}^\bullet$  radicals [25].

The evolution of the characteristic IR bands on thermo-oxidized membrane was similar to the one observed on hypochlorite-treated membrane: decrease of the band at  $1674 \text{ cm}^{-1}$  and appearance of three new bands at  $1034$ ,  $1700$  and  $1770 \text{ cm}^{-1}$ . From these results, we assumed that PES/PVP membrane degrades by radical oxidation.

To validate the assumption that the membrane degradation may be induced by radical attack, a set of hypochlorite ageing tests (pH 8, 350 ppm) was performed with the addition of an excess of a radical scavenger, the 2-methylpropan-2-ol ( $t\text{BuOH}$ ,  $2 \text{ g L}^{-1}$ ) in the soaking bath. This radical trap readily reacts with free radical compounds potentially present in solution [26], slowing down the membrane degradation kinetics if radicals are involved. Membrane samples were characterized by tensile testing and ATR-IR measurements for several hypochlorite doses ranging from 7 to  $93 \text{ g h L}^{-1}$ , results are given in Fig. 12. Regarding the mechanical properties, the addition of  $t\text{BuOH}$  significantly inhibited the membrane embrittlement for the whole range of hypochlorite dose studied (Fig. 12a). At molecular scale, the analysis of the PVP band for an exposure of  $93 \text{ g h L}^{-1}$  with and without  $t\text{BuOH}$  (Fig. 12b), clearly highlights the inhibiting effect of  $t\text{BuOH}$ . Indeed, the PVP band drop is drastically limited with the addition of  $t\text{BuOH}$ . Those results, together with the thermo-oxidation experiments, provide strong indications for a radical induced PVP degradation at pH 8.

### 3.3. Discussion

Ageing of membrane by radical oxidation involving  $\text{HO}^\bullet$  radicals being demonstrated, the maximal degradation observed at pH

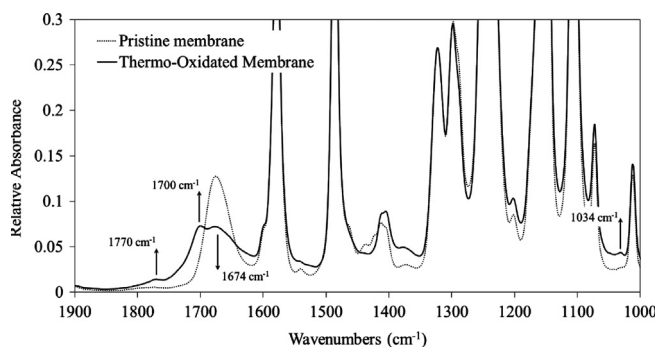
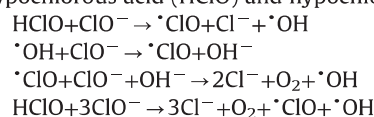


**Fig. 11.** ATR-IR spectra of pristine membrane and membranes treated by thermo-oxidation at  $100^\circ\text{C}$  during 60 days.

8 can be explained. According to Wienk et al., the production of  $\text{HO}^\bullet$  radicals in hypochlorite solution requires the coexistence of hypochlorous acid ( $\text{HClO}$ ) and hypochlorite ion ( $\text{ClO}^-$ ) species [3]:



If we refer to the chlorine dissociation curve presented in Fig. 2, pH 8 value corresponds to a  $\text{HClO}/\text{ClO}^-$  ratio of 1/3, which is precisely the stoichiometric condition for the mechanism leading to free radicals production reported by Wienk et al. The most severe degradation would then occur when  $\text{HClO}$  and  $\text{ClO}^-$  species are non-negligibly present in solution (i.e. for pH 8 and pH 7 values), as it was observed above.

Degradation mechanism being elucidated, question may be raised on the ageing protocols representativeness regarding the actual on-site hypochlorite induced degradation. Two assumptions were made for the design of those experiments: (a) intermittent exposure to hypochlorite over a long period of time is equivalent to a continuous exposure, and (b) the degradation progress is only governed by the hypochlorite dose ( $[\text{TFC}] \times \text{exposure time}$ ) membranes have been exposed to. Regarding the hypochlorite dose, it appears crucial to confirm or reject such an assumption. To this end, we investigated the effect of the [TFC] on the membrane degradation progress. Pristine membranes were immersed in chlorinated water at various concentrations (ppm) during various durations (h) in order to reach the same total dose of  $4000 \text{ ppm h}$  ( $4 \text{ g h L}^{-1}$ ): for example 400 ppm during 10 h and 4000 ppm during 1 h. The degradation of the membranes was then evaluated by the IR-ATR measurement of the relative absorbance of the PVP amide band ( $1674 \text{ cm}^{-1}$ ) and of the PVP oxidation band ( $1700 \text{ cm}^{-1}$ ) as shown in Fig. 13.

Results reported in Fig. 13 clearly demonstrate that for the same total dose quite different effects can be observed at high and low [TFC]. A high concentration significantly increases the oxidation rate compared to a low concentration. Consequently it is not possible to compare two ageings with quite different chlorine concentrations. Nevertheless, one can also observe that for [TFC] of 400 ppm and 800 ppm, membranes underwent the same extent of degradation (same PVP band decrease and no detectable oxidation products) when exposed to the same hypochlorite dose. The assumption that degradation rate is only governed by the hypochlorite dose the membrane is exposed to appears then to be valid on a limited [TFC] range. For high [TFC], the concentration impact on the degradation rate is no longer negligible and has to be taken into account. This is the reason why accelerated ageing experiments using higher concentration and shorter exposure time as compared to on-site operation may overestimate the membrane degradation for the same hypochlorite dose. In our case, the [TFC] of 350 ppm chosen for the study was selected to be within the concentration range encountered during on-site operation (20–400 ppm).

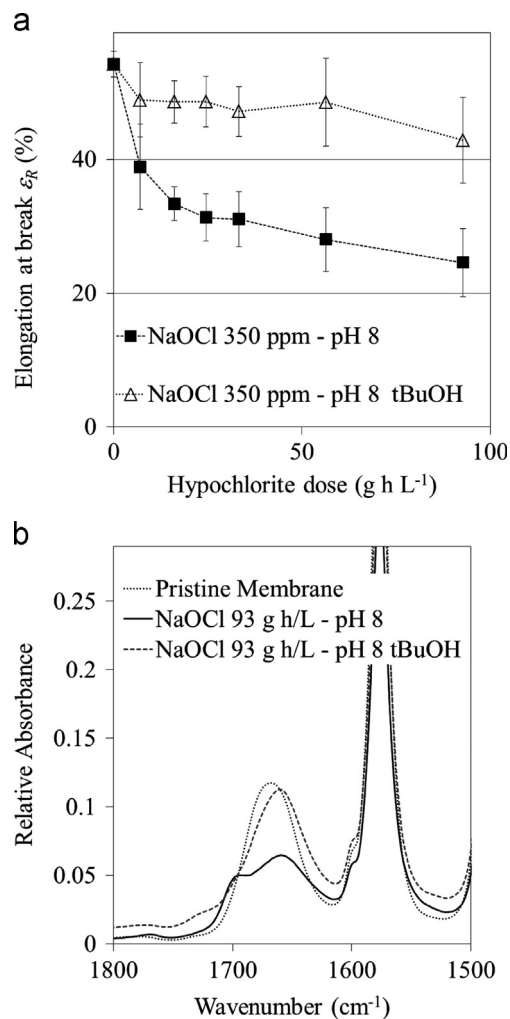


**Fig. 12.** Membrane elongation at break  $\epsilon_R$  as a function of hypochlorite dose when exposed to 350 ppm NaOCl solutions at pH 8, with and without tBuOH (a); ATR-IR spectra of pristine membrane and pH 8 hypochlorite-treated membranes at 93 g h L<sup>-1</sup>, in the presence and in the absence of tBuOH (b).

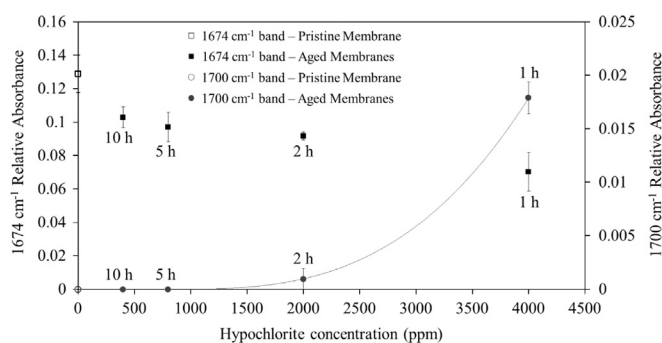


**Fig. 13.** Relative ATR-IR absorbance of the 1674 cm<sup>-1</sup> PVP band and of the 1700 cm<sup>-1</sup> PVP oxidation band measured on membranes exposed to the same hypochlorite dose of 4000 ppm h (4 g h L<sup>-1</sup>), at various [TFC] at pH 8; for each measurement, the contact duration (h) is reported.

Based on the performances modification induced by the contact with hypochlorite solution, results were analyzed to correlate the macroscopic properties to the molecular changes. Pure water permeability  $L_p/\mu_{20}$  is an intrinsic membrane characteristic mainly governed by the size distribution of pores of the selective layer. Dislodgement of PVP from the membrane may also free up access to new pores and enlarge existing pores in the membrane active

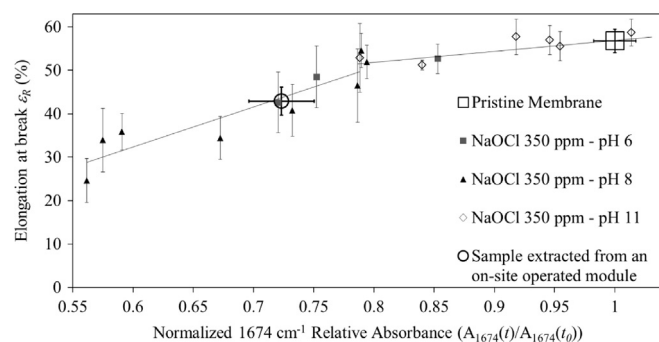


**Fig. 14.** Elongation at break versus PVP normalized IR band relative absorbance for various hypochlorite exposure conditions.

layer, leading to an increase of  $L_p/\mu_{20}$  [27]. For the early stages of the degradation, results shown that the decrease of the PVP IR band corresponds to an increase of  $L_p/\mu_{20}$ , meaning that the PVP removal leads to an increased active layer accessible porosity. As the degradation is more advanced,  $L_p/\mu_{20}$  reaches a plateau (for a lower dose at pH value closer to 8). Assumption is made that beyond a given hypochlorite dose (function of the pH of the solution), the degradation and removal of the majority of the PVP accessible within the selective layer (within a thickness of 10–100 nm) has occurred. This relatively stable state of the membrane skin thus leads to stabilization of the water transfer properties.

Furthermore, it was shown that PVP and PES degradation only occurs in an approximately 30–40  $\mu$ m thick region under the membrane surface, corresponding to the area where PVP is mainly present in the pristine membrane. Since this region also happened to be free of macrovoids and substantially denser than the membrane bulk, it can be thought that its degradation advancement will impact the mechanical resistance of the overall membrane. Fig. 14 presents the changes of elongation at break  $\epsilon_R$  versus the PVP IR band relative absorbance normalized back to the pristine membrane value. A compilation of the data collected at pH 6, 8 and 11 for a wide range of hypochlorite doses is reported. This figure shows that the mechanical properties of the membrane are not significantly altered until the intensity of the 1674 cm<sup>-1</sup> band reaches 80% of its initial value. For lower intensity corresponding to more severe PVP oxidation and/or removal, very severe decrease in elongation at break was observed. At this stage of the degradation, the PVP attack may lead to the outbreak of localized structural weakness. Some of those structural defects might then be considerable enough for facilitating crack propagation.

Autopsy and characterization of similar PES/PVP membranes extracted from an operated industrial module were additionally conducted. In place cleanings of this module were performed using hypochlorite and the module operated over a period of 6 years in a French water production plant. Nevertheless, the exact history of operation, and especially the hypochlorite dose the module was exposed to, is unknown. Samples extracted from the on-site operated module were analyzed by tensile testing and ATR-IR. Results regarding  $\epsilon_R$  and the PVP IR band intensity are reported in Fig. 14. PVP IR band intensity decreases of approximately 28% as compared to the pristine membrane. This decrease goes along with the appearance of the PVP oxidation products at 1700/1770 cm<sup>-1</sup> (not presented here). The relationship between  $\epsilon_R$  and the PVP IR band intensity established by laboratory ageing experiments outstandingly predicted the extent of membrane embrittlement observed for the on-site operated samples. Consequently, it can be concluded that laboratory continuous hypochlorite exposure at 350 ppm and on-site intermittent hypochlorite exposure lead to the same structural and molecular changes of PES/PVP membranes.

#### 4. Conclusion

This study undertook a multi-scale analysis of the degradation of PES/PVP UF hollow fiber membranes when exposed to hypochlorite. It was confirmed that hypochlorite exposure induces PVP radical degradation (involving PVP chain scissions) and dislodgement from the PES matrix, leading to an increase of the pure water permeability and to an embrittlement of the membrane. A direct relationship between elongation at break and PVP IR band intensity changes was established. Advanced chemical analysis brought direct evidence of PES oxidation without chain scission, occurring only within the first 40  $\mu\text{m}$  of the membrane thickness, where PVP is present. It was demonstrated that the presence of PVP and/or PVP degradation products is a required condition for PES oxidation to occur. The first 40  $\mu\text{m}$  of the membrane thickness were also shown to be substantially denser (free of macrovoids) as compared to the membrane bulk.

PVP additive, accounting for a few wt% in the membrane matrix, is then responsible for the membrane integrity loss. In order to maximize the on-site operation lifetime, membrane formulation and processing parameters may be adjusted to facilitate PVP migration and concentration to the active layer and minimize the presence of PVP in the 40  $\mu\text{m}$  thick layer. Since this 40  $\mu\text{m}$  thick layer appears to mainly provide the mechanical resistance of the overall membrane, adjustment of processing parameters may also be done to obtain a less asymmetric membrane structure, with a macrovoids free bulk, exclusively composed of PES polymer.

Hypochlorite exposure conditions and especially the pH were demonstrated to be of crucial importance in the degradation rate. In light of those results, it can be suggested to avoid as much as possible aqueous hypochlorite solutions with pH value between 7 and 8 when performing in-place cleanings.

#### Acknowledgments

Financial support from the French National Research Agency is gratefully acknowledged. Authors are grateful to Aurelien Tournebize for his help with the VITA-AFM analysis.

#### References

- [1] N. Porcelli, S. Judd, Chemical cleaning of potable water membranes: a review, *Separation and Purification Technology* 71 (2010) 137–143.
- [2] A.J. Gijsbertsen-Abrahamse, E.R. Cornelissen, J.A.M.H. Hofman, Fiber failure frequency and causes of hollow fiber integrity loss, *Desalination* 194 (2006) 251–258.
- [3] J. Carrell Morris, The acid ionization constant of HOCl from 5 to 35°, *Journal of Physical Chemistry* 70 (1966) 3798–3805.
- [4] C.G. White, *Handbook of Chlorination and Alternative Disinfectants*, 4th ed., Wiley-Interscience Publication, USA, 1999, 212–287.
- [5] I.M. Wienk, Twente University, NL, 1993. (Ph.D. thesis).
- [6] I.M. Wienk, E.E.B. Meuleman, Z. Borneman, T. Boomgaard, Chemical treatment of membranes of a polymer blend: mechanism of the reaction of hypochlorite with poly(vinyl pyrrolidone), *Journal of Polymer Science* 33 (1995) 49–54.
- [7] J.J. Qin, M.H. Oo, Y. Li, Development of high flux polyethersulfone hollow fiber ultrafiltration membranes from a low critical solution temperature, *Journal of Membrane Science* 247 (2005) 137–142.
- [8] F. Thominet, O. Farnault, E. Gaudichet-Maurin, C. Machinal, J.C. Schrotter, Ageing of polyethersulfone ultrafiltration membranes in hypochlorite treatment, *Desalination* 200 (2006) 7–8.
- [9] E. Arkhangelsky, D. Kuzmenko, V. Gitis, Impact of chemical cleaning on properties and functioning of polyethersulfone membranes, *Journal of Membrane Science* 305 (2007) 176–184.
- [10] E. Arkhangelsky, D. Kuzmenko, N.V. Gitis, M. Vinogradov, S. Kuiry, V. Gitis, Hypochlorite cleaning causes degradation of polymer membranes, *Tribology Letters* 28 (2007) 109–116.
- [11] K. Yadav, K.R. Morison, M.P. Staiger, Effects of hypochlorite treatment on the surface morphology and mechanical properties of polyethersulfone ultrafiltration membranes, *Polymer Degradation and Stability* 94 (2009) 1955–1961.
- [12] K. Yadav, K.R. Morison, Effects of hypochlorite exposure on flux through polyethersulfone ultrafiltration membranes, *Food and Bioprocess Processing* 88 (2010) 419–424.
- [13] S.H. Hamid, *Handbook of Polymer Degradation*, 2nd ed., Marcel Dekker, USA, 2000, 671–698.
- [14] R. Prulho, S. Thérias, A. Rivaton, J.L. Gardette, Ageing of polyethersulfone/polyvinylpyrrolidone blends in contact with bleach water, *Polymer Degradation and Stability* 98.6 (2013) 1164–1172.
- [15] C. Causserand, S. Rouaix, J.P. Lafaille, P. Aimar, Ageing of polysulfone membranes in contact with bleach solution: Role of radical oxidation and of some dissolved metal ions, *Chemical Engineering and Processing: Process Intensification* 47 (2008) 48–56.
- [16] B. Pellegrin, E. Gaudichet-Maurin, C. Causserand, Mechano-chemical ageing of PES/PVP ultrafiltration membranes used in drinking water production, *Water Science and Technology: Water Supply* 13.2 (2013) 541–551.
- [17] S. Rouaix, C. Causserand, P. Aimar, Experimental study of the effects of hypochlorite on polysulfone membrane properties, *Journal of Membrane Science* 277 (2006) 137–147.
- [18] F. Hassouna, S. Therias, G. Mailhot, J.L. Gardette, Photooxidation of poly(N-vinylpyrrolidone) (PVP) in the solid state and in aqueous solution, *Polymer Degradation and Stability* 94 (2009) 2257–2266.
- [19] J.E. Mark, *Polymer Data Handbook*, 1st ed., Oxford University Press, New York, NY, 1999, 962–964.
- [20] K. Sakurai, T. Maegawa, T. Takahashi, Glass transition temperature of chitosan and miscibility of chitosan/poly(N-vinyl pyrrolidone) blends, *Polymer* 41 (2000) 7051–7056.
- [21] H. Xu, S.W. Kuo, J.S. Lee, F.C. Chang, Glass transition temperatures of poly(hydroxystyrene-co-vinylpyrrolidone-co-isobutylstyryl) polyhedral oligosilsesquioxanes, *Polymer* 43 (2002) 5117–5124.
- [22] J.E. Mark, *Polymer Data Handbook*, 1st ed., Oxford University Press, New York, NY, 1999, 480–482.
- [23] T. Sasuga, H. Kudoh, T. Seguchi, High energy ion irradiation effects on polymer materials—changes in mechanical properties of PE, PSF and PES, *Polymer* 40 (1999) 5095–5102.
- [24] Y. Li, T.S. Chung, C. Cao, S. Kulprathipanja, The effects of polymer chain rigidification, zeolite pore size and pore blockage on PES-zeolite: a mixed matrix membranes, *Journal of Membrane Science* 260 (2005) 45–55.
- [25] V.V. Krongauz, M.T.K. Ling, Photo-crosslinked acrylates degradation kinetics, *Journal of Thermal Analysis and Calorimetry* 96 (2009) 715–725.
- [26] J. Staehelin, J. Hoigné, Decomposition of ozone in water in the presence of organic solutes acting as promoters and inhibitors of radical chain reactions, *Environmental Science and Technology* 19 (1985) 1206–1213.
- [27] S.H. Wolff, A.L. Zydney, Effect of bleach on the transport characteristics of polysulfone hemodialyzers, *Journal of Membrane Science* 243 (2004) 389–399.